



Modeling of the magnetic chemically peculiar star HD 188101

R. Bayazitov¹ and L. Mashonkina²

¹ Kazan Federal University, 18 Kremlyovskaya, Kazan, 420008 Russia

² Institute of Astronomy of the Russian Academy of Sciences, 48 Pyatnitskaya, Moscow, 119017 Russia

Abstract. We present the study of the He-weak star HD 188101. Using spectral observations obtained with the Main stellar spectrograph (MSS) and the Nasmyth echelle spectrograph (NES) mounted on the BTA SAO RAS and the data from the literature, we determined the fundamental parameters: $T_{\text{eff}} = 15\,600 \pm 400$ K, $\log g_{\text{spec}} = 3.87 \pm 0.13$, $R = 2.1\text{--}3.1 R_{\odot}$, $M = 3.8\text{--}4.8 M_{\odot}$. Chemical abundances were determined by the synthetic spectrum method: under the LTE assumption for He, N, Ti, Fe and without LTE for C, O, Mg, Si. For Si and Fe, overabundance of about 0.6 dex relative to the solar abundance was found. The non-LTE calculations with the stellar Si abundance lead to consistent abundances from lines of Si II and Si III, while the difference between LTE abundances amounts to 0.8 dex.

Keywords: stars: chemically peculiar, abundances, atmospheres, magnetic fields

DOI: 10.26119/VAK2024.047

1 Introduction

Chemically peculiar stars make up about 10–20% of B–A type stars of the main sequence. They show deficiency or excess in abundance of some elements relative to the solar abundance. Since atmospheres of B–A type stars are non-convective, the selective diffusion of chemical elements is possible (Michaud 1970) in case of the slow rotation as observed for CP stars. Large-scale magnetic field detected in many CP stars additionally stabilizes the atmosphere and leads to periodic variations in the star’s brightness and in the profiles of some spectral lines. These variations are explained by chemical spots on the stellar surface associated with the magnetic field.

From analysis of the Kepler’s light curves Hümmerich et al. (2018) selected new candidate CP stars. These stars became targets of a spectropolarimetric monitoring on the 6-m telescope BTA. The results for 10 objects are presented by Yakunin et al. (2023). The hottest star of this sample, HD 188101, was selected for the present study. The star has the sinusoidal light curve and a poorly approximated dependence of the longitudinal magnetic field on the phase. Effective temperature of HD 188101 was estimated as $T_{\text{eff}} = 14\,700$ K and the surface gravity as $\log g = 3.8$. It was noted that at the local thermodynamic equilibrium (LTE) assumption effective temperatures of 15 200 K and 17 200 K are needed to reproduce the Si II and Si III lines respectively. The He I $\lambda 4471$ line profile cannot be reproduced.

In this work we determine the fundamental parameters of HD 188101, abundances of He, C, N, O, Mg, Si, Ti, Fe at the LTE assumption, a type of chemical peculiarity of the star and investigate the non-LTE (NLTE) effects for the C II, O I, Mg II, Si II and Si III lines.

2 Observations

We use spectra obtained in 2019 and 2020 with the Main stellar spectrograph (MSS) of the BTA. Spectral resolving power is $R = \lambda/\Delta\lambda \approx 15\,000$, the signal-to-noise ratio is $S/N = 150\text{--}200$, the spectral range covers 4450–5000 Å. We also use the spectrum from the Nasmyth echelle spectrograph (NES) of the BTA obtained in 2019 with $R = 50\,000$, $S/N = 50$, spectral range of 3950–6880 Å. The phases were obtained from the periodogram: $\text{JD} = 2455681.4953 + 3.98726E$. We use the parallax obtained by the HIPPARCOS mission and updated later (HIP2007, van Leeuwen 2007) $\pi = 2.82 \pm 0.50$ mas, and the Gaia measurements (Gaia DR3, Gaia Collaboration et al. 2021) $\pi = 2.34 \pm 0.10$ mas.

Photometric data were extracted from the VizieR portal¹ for comparison with a theoretic spectral energy distribution (SED).

¹ <https://vizier.cds.unistra.fr/viz-bin/VizieR>

3 Fundamental parameters of HD 188101

Interpolation along T_{eff} is carried out in the grid of fluxes calculated by Castelli & Kurucz (2003) to describe the observed fluxes. An angular diameter of the star θ is derived from the infrared flux method (IFRM) using effective wavelengths from $1 \mu\text{m}$ to $13 \mu\text{m}$. The color excess $E(B-V) = 0.08$ is taken from Gontcharov (2017). The best agreement with observations (Fig. 1) was obtained with $T_{\text{eff}} = 15500 \pm 500 \text{ K}$, $\log g = 4.0$, $[M/H] = 0.0$, $\theta = 0.066 \text{ mas}$. The uncertainty in T_{eff} was estimated from the TD1 data spread.

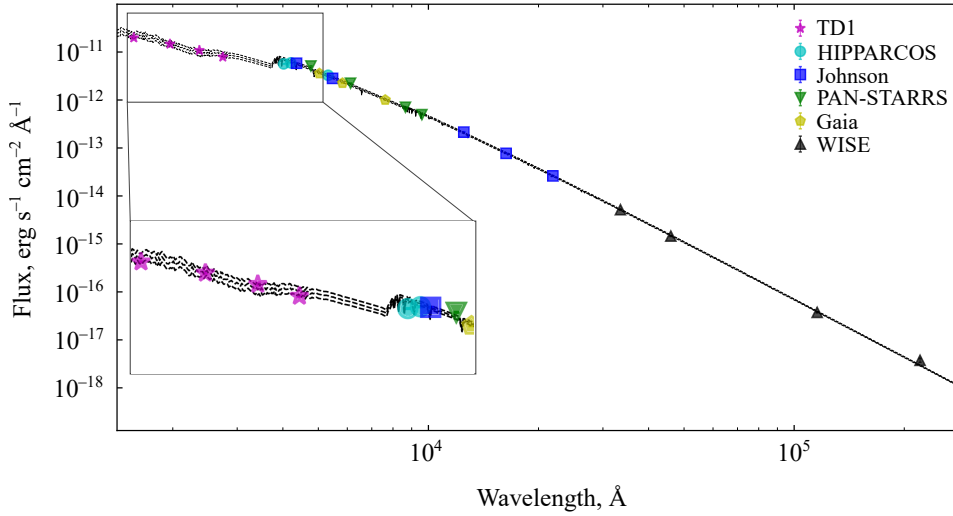


Fig. 1. The observational data of HD 188101 are shown by different type symbols. Synthetic spectra for the models with $T_{\text{eff}} = 15500 \pm 500 \text{ K}$, $\log g = 4.0$, $[M/H] = 0.0$, $\theta = 0.066 \text{ mas}$ are shown by the lines.

Based on the stellar parallax, evolutionary tracks (Dotter 2016), obtained T_{eff} and θ , we conclude that HD 188101 is located near the zero age main sequence, has the mass M and $\log g_{\text{phot}}$ indicated in Table 1.

Using the non-LTE synthetic spectra (Lanz & Hubeny 2007), we constrain $\log g_{\text{spec}}$ and T_{eff} from fitting the $H\beta$ line profile in the MSS spectrum: $\log g_{\text{spec}}$ varies from 3.75 to 4.0 and T_{eff} from 15000 K to 16000 K. Similar atmospheric parameters of $T_{\text{eff}} = 15610 \pm 440 \text{ K}$, $\log g = 3.96 \pm 0.06$ were obtained using the SME software package (LTE assumption Valenti & Piskunov 1996; Piskunov & Valenti 2017), grid of the LLmodels model atmospheres (Shulyak et al. 2004) and VALD3² atomic data

² <http://vald.inasan.ru>

base (Ryabchikova et al. 2015). Our analysis is made with the 15 600/4.0/0.0 model atmosphere.

Table 1. The fundamental parameters of HD 188101.

Parameter	Quantity	Method
θ , mas	0.066	IFRM
R , R_{\odot} (HIP2007)	2.52 ± 0.45	IFRM
R , R_{\odot} (Gaia EDR3)	3.03 ± 0.12	IFRM
$\log g_{\text{phot}}$ (HIP2007)	4.1–4.4	Evolutionary tracks
$\log g_{\text{phot}}$ (Gaia EDR3)	4.05–4.20	Evolutionary tracks
M , M_{\odot}	3.8–4.8	Evolutionary tracks
$\log g_{\text{spec}}$	3.75–4.00	H β
T_{eff} , K	$15\,600 \pm 400$	Photometry + H β

4 Chemical abundances

Strong lines of Si II, Si III, Fe III, Ti II and weak lines of He I are observed in the MSS spectrum. All the lines of Si II, Si III, Ti II and the strongest magnesium line, Mg II $\lambda 4481$, show profile variations. Variations in the He I $\lambda 4713$ profile amount to 20%. We note that the strongest line of Al II $\lambda 4663$ cannot be detected in the NES spectrum.

NLTE calculations for C I–II, O I, Mg I–II, Si I–II–III were made with the `DETAIL` code (Giddings 1981; Butler 1984; Przybilla et al. 2011) using model atoms described by Sitnova et al. (2004); Alexeeva et al. (2021, 2018) and Mashonkina (2020). Departure coefficients for the atomic levels calculated in the `DETAIL` are implemented into the `SYNTHV_NLTE` code (Tsymbal et al. 2019). Using the `Binmag6` code (Kochukhov 2018), `SYNTHV_NLTE` allows us to fit observations. Atomic data for spectral lines were obtained from the VALD data base. Model atmospheres were calculated with the `LLmodels` code.

NLTE corrections for the Mg II lines range from -0.19 to 0.08 dex, those of the C II lines do not exceed 0.01 dex. For the Si II lines with an excitation energy of the lower level from 8.12 eV to 12 eV, the NLTE corrections reach 1.0 dex. The NLTE corrections for another Si II lines do not exceed 0.7 dex. The NLTE calculations with $[\text{Si}/\text{H}] = 0.6$ and $[\text{Si}/\text{H}] = 0.0$ lead to different NLTE effects for Si II. We note that the Si II $\lambda 6239$ line profile is reproduced and the Si II/Si III ionization equilibrium is achieved when $[\text{Si}/\text{H}] = 0.6$ dex is used in the NLTE calculations. For the Si III lines, the NLTE corrections range from -0.10 dex to -0.25 dex.

The obtained average abundances $[N_{\text{el}}/N_{\text{tot}}]$ are presented in Fig. 2. Solar abundances were taken from Asplund et al. (2021). The root mean square error is calculated as a standard deviation $\sigma = \sqrt{\sum(x - \bar{x})^2 / (N_l - 1)}$, where N_l is the number of lines. The abundance of oxygen is determined with large uncertainty due to defects in the spectrum near the O I $\lambda 6155$, $\lambda 6158$ lines. The solar abundance was obtained from the Mg II $\lambda 4427$, $\lambda 4433$ lines. But the Mg II $\lambda 4481$ line gives a lower abundance, by 0.5 dex. This discrepancy requires further research.

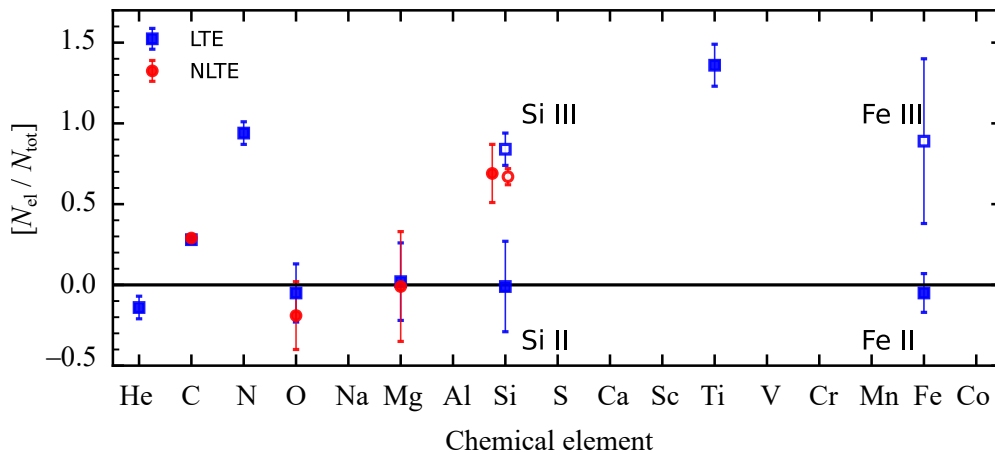


Fig. 2. Stellar chemical abundances relative to the solar ones are obtained from the NES and the MSS (2019.11.17) spectra. Abundances determined from the Fe III and Si III lines are shown by the open symbols. Here $[N_{\text{el}}/N_{\text{tot}}] = \log(N_{\text{el}}/N_{\text{tot}})_{\text{star}} - \log(N_{\text{el}}/N_{\text{tot}})_{\text{Sun}}$.

5 Summary

Based on the analysis of spectroscopic and photometric data, the following results were obtained for the CP star HD 188101.

1. We determined the fundamental parameters: $T_{\text{eff}} = 15\,600 \pm 400$ K and $\log g_{\text{spec}} = 3.87 \pm 0.13$. Surface gravity $\log g_{\text{spec}}$ based on fitting the $H\beta$ line profile is less by 0.2 dex than $\log g_{\text{phot}}$ determined from the evolutionary tracks.
2. Abundances of He, C, N, O, Mg, Si, Ti, Fe were determined with the LTE assumption and without LTE for C, O, Mg, Si. Our analysis finds enhanced abundances of N, Si, Ti, Fe relative to the solar abundances, by about 0.6 dex, and depleted abundance of He. The other elements reveal solar abundances, within 0.2 dex.

HD 188101 is a CP star of a CP4 He-weak, Si type according to the classification proposed by Preston (1974).

3. A difference of 0.85 dex in the LTE abundances between the Si II and Si III lines is removed in the NLTE calculations with $[\text{Si}/\text{H}] = 0.6$ characteristic of HD 188101. No signatures of Si stratification in the atmosphere of HD 188101 is found. With the LTE assumption, an abundance difference was also found between lines of Fe II and Fe III. NLTE calculations for Fe II–Fe III are needed to study the sources of such a difference.

References

- Alexeeva S., Ryabchikova T., Mashonkina L., et al., 2018, *Astrophysical Journal*, 866, 2, id. 153
 Alexeeva S., Ryabchikova T., Mashonkina L., 2021, *Monthly Notices of the Royal Astronomical Society*, 462, 1, p. 1123
 Asplund M., Amarsi A., Grevesse N., 2021, *Astronomy & Astrophysics*, 653, id. A141
 Butler K., 1984, Ph.D. Thesis, University of London
 Castelli F. and Kurucz R.L., 2003, *IAU by the Astronomical Society of the Pacific*, 210, p. A20
 Dotter A., 2016, *Astrophysical Journal Supplement Series*, 222, 1, id. 8
 Gaia Collaboration, Brown A.G.A., Vallenari A., et al., 2021, *Astronomy & Astrophysics*, 649, id. A1
 Giddings J.R., 1981, Ph.D. Thesis, University of London
 Gontcharov G.A., 2017, *Astronomy Letters*, 43, 7, p. 472
 Hümmerich S., Mikulášek Z., Paunzen E., et al., 2018, *Astronomy & Astrophysics*, 619, id. A98
 Kochukhov O., 2018, *Astrophysics Source Code Library*, record ascl:1805.015
 Lanz T. and Hubeny I., 2007, *Astrophysical Journal Supplement Series*, 169, 1, p. 83
 van Leeuwen F., 2007, *Astronomy & Astrophysics*, 474, 2, p. 653
 Mashonkina L., 2020, *Monthly Notices of the Royal Astronomical Society*, 493, 4, p. 6095
 Michaud G., 1970, *Astrophysical Journal*, 160, p. 641
 Piskunov N. and Valenti J.A., 2017, *Astronomy & Astrophysics*, 597, id. A16
 Preston G.W., 1974, *Annual Review of Astronomy and Astrophysics*, 12, p. 257
 Przybilla N., Nieva M.-F., Butler K., 2011, *Journal of Physics Conference Series*, 328, 1, id. 012015
 Ryabchikova T., Piskunov N., Kurucz R.L., et al., 2015, *Physica Scripta*, 90, 5, id. 054005
 Shulyak D., Tsymbal V., Ryabchikova T., et al., 2004, *Astronomy & Astrophysics*, 428, p. 993
 Sitnova T.M., Mashonkina L.I., Ryabchikova T.A., 2004, *Astronomy Letters*, 39, 2, p. 126
 Tsymbal V., Ryabchikova T., Sitnova T., 2019, *ASP Conference Series*, 518, p. 247
 Valenti J. and Piskunov N., 1996, *Astronomy and Astrophysics Supplement*, 118, p. 595
 Yakunin I., Semenko E., Romanyuk I., et al., 2023, *Astrophysical Bulletin*, 78, 2, p. 141